

Structure, Equilibrium and Ribonuclease Activity of Copper(II) and Zinc(II) Complexes Formed with a Dinucleating Bis-Imidazole Ligand

Tamás Gajda,^{*,[a],[b]} Roland Krämer,^[b] and Attila Jancsó^[a]

Keywords: Enzyme models / Hydrolyses / Phosphodiesterases / Copper / Zinc

The syntheses, crystal structures, solution equilibria and ribonuclease activity are reported for copper(II) and zinc(II) complexes of a new potentially dinucleating, bis-imidazole ligand *N,N'*-bis(5-methylimidazol-4-ylmethyl)-1,3-diaminopropan-2-ol (**bimido**). The zinc(II) ion in $[\text{Zn}(\text{bimido})\text{Cl}]\text{NO}_3$ is coordinated in a slightly distorted square pyramidal environment, with the four N atoms of bimido in the basal positions and the Cl[−] ion in the axial one. The two copper(II) ions in $[\text{Cu}_2(\text{bimido}_{-1\text{H}})(\text{DPP})(\text{ClO}_4)(\text{CH}_3\text{OH})]\text{ClO}_4 \cdot 1/2 \text{H}_2\text{O}$ (DPP = diphenyl phosphate) are bridged by the deprotonated alkoxo group of bimido and by the phosphate group of DPP in a 1,3-bridging mode. Depending on the [M]/[L] ratio, the ML and $\text{M}_2\text{L}_{-2\text{H}}$ species are present in solution in the neutral pH range, having analogous structures as described above for the crystalline complexes. The zinc(II)-bimido (2/1) sys-

tem, in a 65% EtOH-H₂O mixed solvent, shows an important increase of hydrolytic activity, parallel with the formation of the $\text{Zn}_2\text{L}_{-2\text{H}}$ species, with a sigmoidal pH-rate profile modelling both steps of RNA hydrolysis. The k_{cat} value for the transesterification of 2-hydroxypropyl-*p*-nitrophenyl phosphate by $\text{Zn}_2\text{L}_{-2\text{H}}$, determined from saturation kinetic measurements ($T = 298 \text{ K}$), corresponds to a maximum rate acceleration ($k_{\text{cat}}/k_{\text{uncat}}$) of ca. 10^4 . The observed pseudo-first order rate constant for the hydrolysis of uridine 2',3'-cyclic monophosphate, under nearly physiological conditions ($T = 310 \text{ K}$, pH = 8, $[\text{Zn}_2\text{L}_{-2\text{H}}] = 3.6 \text{ mM}$, $k_{\text{obs}} = 2 \cdot 10^{-5} \text{ s}^{-1}$) reflects a higher hydrolytic activity of $\text{Zn}_2\text{L}_{-2\text{H}}$ towards this biologically relevant substrate ($k_{\text{obs}}/k_{\text{uncat}}$ indicates ca. 10^4 fold rate acceleration). The proposed mechanisms include bifunctional Lewis-acid and general base catalysis.

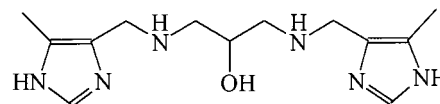
Introduction

The fundamental role of the imidazole moiety in the active centre of a large number of metalloproteins is well established. During the past two decades a wide variety of imidazole-containing ligands have been investigated to mimic structural features of these enzymes, but less attention was devoted to functional mimicking. The presence of an imidazole moiety in the catalytic centres of enzymes is often related to hydrolytic reactions. Phosphoesterases are responsible for the hydrolysis of phosphate esters and are involved in a number of biological processes. Nucleases are an important class of these enzymes and are used in the repair and hydrolysis of DNA and RNA, as well as in viral defence (restriction enzymes).

Low molecular weight functional model complexes of phosphoesterases have attracted great interest due to their possible application in biotechnology, molecular biology and chemotherapy. A number of metalloenzymes that hydrolyse phosphate esters are activated by two or more cooperating metal ions.^[1] The possible cooperative effect of the bimetallic core on the hydrolysis of phosphoesters has

inspired a number of model studies dealing with dinuclear complexes.^[2–14] Mechanistic features of some low molecular weight model complexes show notable similarities to the mechanism proposed for certain dinuclear phosphoesterases,^[2] in particular the μ -1,3 bridging of the phosphoester substrate combined with nucleophilic attack of metal-bound hydroxide. Although important rate acceleration of phosphate ester hydrolysis has been demonstrated in many cases, only a few reflect on the catalytic centres of the native phosphoesterases, from both a structural and functional point of view.

As an extension of our study on coordination chemistry of the imidazole ring,^[14–17] we report here the syntheses, crystal structures, solution equilibria and ribonuclease activity of copper(II) and zinc(II) complexes formed with a new multidentate, bis-imidazole ligand *N,N'*-bis(5-methylimidazol-4-ylmethyl)-1,3-diaminopropan-2-ol (**bimido**, Scheme 1).



Scheme 1. Schematic structure of bimido

Our aim was to design a dinucleating imidazole ligand which provides a relatively open coordination environment for the bound metal ions and an alkoxo-bridge which holds them relatively close to each other, allowing the metal-metal cooperation in the binding and the hydrolysis of phosphoesters. In the presence of an excess of metal ($[\text{Zn}]/[\text{L}] = 2/1$), the zinc(II)-bimido system was indeed found to be an

^[a] Department of Inorganic and Analytical Chemistry, University of Szeged
6701 Szeged, P.O. Box 440, Hungary,
Fax: (internat.) +36/62-420-505,
E-mail: tamas.gajda@chem.u-szeged.hu

^[b] Anorganisch-Chemisches Institut der Universität, Wilhelm-Klemm Straße 8, 48149 Münster, Germany

Supporting information for this article is available on the WWW under <http://www.wiley-vch.de/home/eurjic> or from the author.

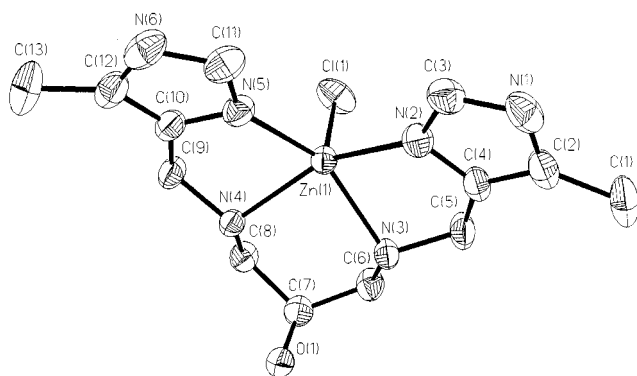


Figure 1. ORTEP view (50%) of **1** with the atom-labelling scheme. Hydrogen atoms and nitrate ions are omitted for clarity

efficient accelerator, modelling both steps of RNA hydrolysis: transesterification of 2-hydroxypropyl-*p*-nitrophenyl phosphate (hnpn) and hydrolysis of uridine 2',3'-cyclic monophosphate (2',3'-cUMP).

Results and Discussion

Description of the Crystal Structures

a. [Zn(bimido)Cl]NO₃ (**1**)

The molecular structure of **1** is shown in Figure 1, selected bond lengths and angles are given in Table 1. The zinc(II) ion in complex **1** is coordinated in a slightly distorted square pyramidal environment, with the four N atoms of bimido in the basal positions and the Cl[−] ion in the axial one. The zinc(II) ion is displaced by 0.527(1) Å from the least-square plane defined by N(2), N(3), N(4) and N(5). The O(1) oxygen of the alcohol is not coordinated to the metal ion. Several hydrogen bonds between the hydrogens on O(1), N(1), N(3) and the nitrate oxygens stabilise the crystal structure. In addition, two complex molecules are linked by a moderately strong hydrogen bonding interaction between the hydrogen on N(6) and O(1) (−*x*, *y*−1/2, *z*+1/2) with an N(6)–O(1) bond length of 2.802 Å.

The penta-coordinated zinc(II) ion is less common in biological systems, but may be relevant to the catalytic reaction intermediates.^[18] Although several square pyramidal zinc(II) complexes are known for linear or cyclic tetraaza ligands,^[19] only a few examples can be found for imidazole derivatives.^[20]

The average Zn–N_{im} distance (2.05 Å) is considerably shorter than the corresponding distance of the secondary

Table 1. Selected interatomic bond lengths (Å) and angles (°) for [Zn(bimido)Cl]NO₃ (**1**)

Zn–N(2)	2.072(2)	Zn–N(4)	2.167(2)
Zn–N(3)	2.132(2)	Zn–N(5)	2.031(2)
Zn–Cl(1)	2.261(1)		
N(2)–Zn–N(3)	79.35(8)	N(4)–Zn–N(5)	78.34(8)
N(2)–Zn–N(4)	151.74(8)	N(2)–Zn–Cl(1)	108.92(7)
N(2)–Zn–N(5)	101.17(8)	N(3)–Zn–Cl(1)	102.60(7)
N(3)–Zn–N(4)	86.53(8)	N(4)–Zn–Cl(1)	97.95(7)
N(3)–Zn–N(5)	148.02(8)	N(5)–Zn–Cl(1)	107.25(7)

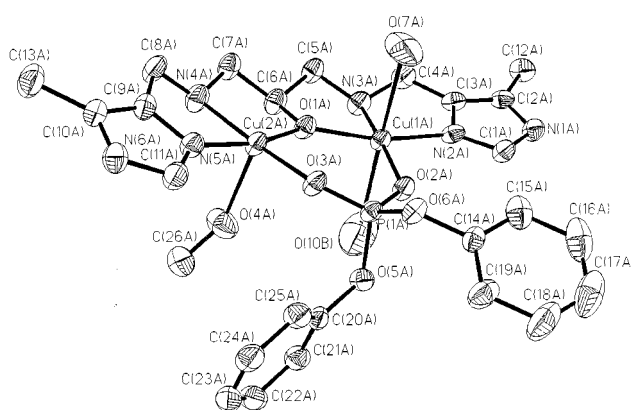


Figure 2. ORTEP view (30%) of **2** with the atom-labelling scheme. Hydrogen atoms and perchlorate ions (except of O(7A) and O(10B)) are omitted for clarity

amines (2.15 Å). The former value (Zn–N_{im}) is also somewhat shorter than the corresponding distance in the only available square pyramidal zinc(II) complex with basal imidazole coordination (2.08 Å).^[20]

The largest distortion in complex **1** from the ideal square pyramidal structure is in the N2–Zn–N5 angle, which is 101.2° (Δ = 15.2°). This is due to the presence of the two fused 5-membered chelate rings in complex **1**, having N–Zn–N angles less than 80°.

b. [Cu₂(bimido-_{1H})(DPP)(ClO₄)(CH₃OH)]ClO₄·1/2H₂O (**2**)

The complex crystallises with two identical dinuclear cations, four perchlorates and a lattice water per unit cell. The molecular structure of **2** is shown in Figure 2, while selected bond lengths and angles are provided in Table 2. The dinuclear complex consists of two distinct copper(II) centres, one is five (4+1) coordinated, the other is six (4+2) coordinated and they are doubly bridged by the alkoxide oxygen of bimido and by the phosphate oxygens of DPP in a 1,3-bridging mode. The five coordinated Cu(2) has a slightly distorted square-pyramidal geometry. The basal plane of Cu(2) is determined by the N(1), N(2), O(1) atoms of bimido in addition to the O(2) oxygen of DPP, while a non-

Table 2. Selected interatomic bond lengths (Å) and angles (°) for [Cu₂(bimido-_{1H})(DPP)(ClO₄)(CH₃OH)]ClO₄·1/2 H₂O (**2**)

Cu(1)–O(1)	1.901(4)	Cu(2)–O(1)	1.881(4)
Cu(1)–O(2)	1.915(4)	Cu(2)–O(3)	1.916(4)
Cu(1)–N(2)	1.929(5)	Cu(2)–N(4)	2.001(5)
Cu(1)–N(3)	1.999(5)	Cu(2)–N(5)	1.921(5)
Cu(1)–O(7)	2.540(7)	Cu(2)–O(4)	2.361(6)
Cu(1)–O(10) ^[a]	2.57(1)	Cu(1)–Cu(2)	3.493(2)
O(1)–Cu(1)–O(2)	98.5(2)	O(1)–Cu(2)–O(3)	97.4(2)
O(1)–Cu(1)–N(2)	165.1(2)	O(1)–Cu(2)–N(5)	166.7(2)
O(2)–Cu(1)–N(2)	94.8(2)	O(3)–Cu(2)–N(5)	94.1(2)
O(1)–Cu(1)–N(3)	84.3(2)	O(1)–Cu(2)–N(4)	85.9(2)
O(2)–Cu(1)–N(3)	171.6(2)	O(3)–Cu(2)–N(4)	173.3(2)
N(2)–Cu(1)–N(3)	83.5(2)	N(5)–Cu(2)–N(4)	82.0(2)
O(1)–Cu(1)–O(7)	85.5(2)	O(1)–Cu(2)–O(4)	88.9(2)
O(2)–Cu(1)–O(7)	89.7(3)	O(3)–Cu(2)–O(4)	99.8(2)
N(2)–Cu(1)–O(7)	87.9(3)	N(5)–Cu(2)–O(4)	95.9(2)
N(3)–Cu(1)–O(7)	98.4(3)	N(4)–Cu(2)–O(4)	86.0(3)
		Cu(2)–O(1)–Cu(2)	134.9(2)

^[a] Symmetry transformation: *x* + 1, *y*, *z*.

deprotonated methanol oxygen is coordinated in the apical position ($\text{Cu}-\text{O} = 2.359 \text{ \AA}$). The six coordinated Cu(1) has the same donors in the tetragonal plane (N(3), N(4), O(1) and O(3)), but both axial positions are occupied by loosely bound perchlorate oxygens with a $\text{Cu}-\text{O}$ distance of $\approx 2.54 \text{ \AA}$. As a result, the $\text{Cl}(1)\text{O}_4^-$ perchlorate ion bridges two neighbouring dinuclear complexes, forming an infinite chain within the crystal. This structural motif has been found in only a few dicopper complexes.^[21b] In fact, the oxygen atoms of the methanol and perchlorate ion interact weakly with the metallic orbitals, as a result of the Jahn–Teller effect. The lattice water occupies a special position ($x = 0.5, y = 0.5, z = 0.5$). The interatomic distances between the water oxygen (O(15)) and the other non-hydrogen atoms are all $\geq 3.88 \text{ \AA}$.

The bond lengths in the tetragonal planes of the copper ions ($\text{Cu}-\text{N}_{\text{im}} = 1.927$ and 1.920 , $\text{Cu}-\text{N}_{\text{am}} = 1.997$ and 2.002 , $\text{Cu}-\text{O}_{\text{alc}} = 1.901$ and 1.880 , $\text{Cu}-\text{O}_{\text{P}} = 1.915$ and 1.917 \AA) are similar for the two metal centres. The $\text{Cu}-\text{N}$ distances are, however, considerably shorter ($\Delta = 0.05\text{--}0.15 \text{ \AA}$) relative to the structurally similar tri- or tetra-substituted (benz)imidazole derivatives of 1,3-diamino-2-propanol.^[21] This is probably due to the less distorted tetragonal plane in **2**. On the other hand, the $\text{Cu}-\text{O}$ distances are typical as compared with the related dinuclear complexes.

The $\text{Cu}(1)-\text{Cu}(2)$ distance and the $\text{Cu}(1)-\text{O}(1)-\text{Cu}(2)$ angle in **2** are 3.493 \AA and 134.9° , respectively. These relatively large values are due to the constraint caused by the fused 5-membered chelate rings of the ligand backbone and are in the range obtained for similar complexes of substituted 1,3-diamino-2-propanol ligands.^[21,22] The metal-metal separation and the μ -1,3 bridging fashion of the phosphodiester DPP in **2** is related with many dinuclear metallo-phosphoesterases.^{[1][2a]} The double Lewis activation of phosphodiester achieved in this way is certainly a key feature concerning the observed hydrolytic activity of **2** (see later).

The least square calculation revealed only minor distortion of the basal plane of Cu(2), but the donor atoms are considerably deviated (average deviation 0.133 \AA) from the best plane of Cu(1). As a consequence of the different geometry, only Cu(2) is displaced considerably (0.1 \AA towards O(4)) from its basal plane. The angle between the two least-square planes of the copper(II) centres is $9.4(1)^\circ$ and between the best plane of the $\text{Cu}_2\text{O}_3\text{P}$ unit and the basal plane of Cu(2) is $7.8(1)^\circ$. These facts result in an essentially planar structure of the complex cation.

Finally, several hydrogen bonds, e.g. between N(6)–H and O(11); N(3)–H and O9 ($x+1, y, z$); O(4)–H and O8 ($x+1, y, z$), stabilise the crystal structure.

Complex Formation in Aqueous Solution

The determined protonation and complex formation constants are listed in Table 3 together with some derived data. The two imidazole rings of bimido have $\text{p}K$ values that are ca. one log unit higher than that of the structurally similar N,N' -bis(imidazol-4-ylmethyl)-1,2-ethanediamine^[23] (bi-

Table 3. Logarithmic formation constants for copper(II) and zinc(II) complexes of bimido ($T = 298 \text{ K}$, $I = 0.1 \text{ M}$ (NaClO_4) in water and $I = 0.05 \text{ M}$ (sodium benzenesulfonate) in a 65% (w/w) ethanol–water mixture); $\beta_{\text{pqr}} = [\text{M}_\text{p}\text{L}_\text{q}\text{H}_\text{r}]/[\text{M}][\text{L}]^q[\text{H}]^r$, with estimated errors in parentheses (last digit)

pqr zinc(II)	water copper(II)	zinc(II)	65% (w/w) EtOH–H ₂ O
011	9.055(4)		8.49(1)
012	16.586(4)		15.20(1)
013	21.722(6)		19.35(2)
014	26.074(6)		22.87(2)
111	13.83(5)	–	14.43(2)
110	9.63(1)	18.97(1)	10.97(1)
11–1	0.10(1)	7.81(1)	1.19(3)
21–2	–	–	–0.37(1)
21–3	–	–	–10.38(3)
$\text{p}K_{11}^{10}$	9.53	11.16	9.86
$\log K_{\text{ML},\text{corr}}$	–16.44	–7.10	–11.90
$\text{p}K_{21}^{31}$	–	–	10.01
$\text{NP}^{[a]}(\text{FP}^{[b]})$	366(0.005 cm^{-3})	340(0.004 cm^{-3})	723(0.008 cm^{-3})

[a] NP: number of experimental points. – [b] FP: fitting parameter.

meda, $\text{p}K = 3.21$ and 4.26), probably due to the electron-donating methyl groups on the imidazole rings.

In the presence of zinc(II) the same species are formed in both $[\text{Zn}]/[\text{L}] = 1/1$ and $1/2$ systems. Complex formation starts at pH 4, with the formation of the 3N-coordinated MLH species (Figure 3A). The succeeding ZnL complex is the unique species in the neutral pH region. Its formation at slightly acidic pH suggests 4N coordination in this complex, which is, in fact, proven by X-ray analysis. At higher pH further base consumption is observed ($\text{p}K = 9.53$) which can be assigned to the deprotonation of a metal-bound water molecule (the formation of a metal-coordinated alkoxide anion is less likely due to steric reasons).

In the presence of the copper(II) ion ($[\text{Cu}]/[\text{L}] = 1/1$ or $1/2$) only the CuL and $\text{CuL}_{-1\text{H}}$ complexes are detected in the whole pH range. The formation of the CuL species is complete at pH 4. This fact, together with the spectroscopic parameters determined for this complex ($g_{\perp} = 2.057$, $g_{\parallel} = 2.221$, $A_{\parallel} = 0.0190 \text{ T}$, $g_o = 2.112$, $A_o = 0.0079 \text{ T}$, $\lambda_{\text{max}}^{\text{d-d}} = 570 \text{ nm}$), strongly suggest a 4N coordination in the equatorial plane of copper(II) in CuL. The presence of imidazole rings in bimido results in a rather high stability. The basicity corrected stability constants of the ML complex ($\log K_{\text{ML},\text{corr}} = \log \beta_{110} - \log \beta_{014} = -7.1$ and -16.44 for Cu^{II} and Zn^{II} , respectively) are ca. 2–4 orders of magnitude higher than those of the 1,4,8,11-tetraazaundecane.^[24] Similarly, the existence of the fused chelates causes significant stabilisation relative to the complexes of the strongly related 4-aminomethylimidazole (e.g. $\log K_{\text{CuL2},\text{corr}} = -11.0$,^[25] $\Delta \log K_{\text{corr}} = 3.9$). The deprotonation, leading to the $\text{CuL}_{-1\text{H}}$ species, occurs at $\text{p}K = 11.16$. The observed slight change in the EPR parameters during this process ($g_o = 2.109$, $A_o = 0.00806 \text{ T}$) indicates only minor variations in the coordination sphere of copper(II), i.e. deprotonation of the non-coordinating imidazole-N1 nitrogen. The observed high $\text{p}K$ value agrees well with those obtained for analogous systems.^[17]

Our intention was to achieve dinuclear complexes of bimido, but the solubility of the complexes formed at $2/1$

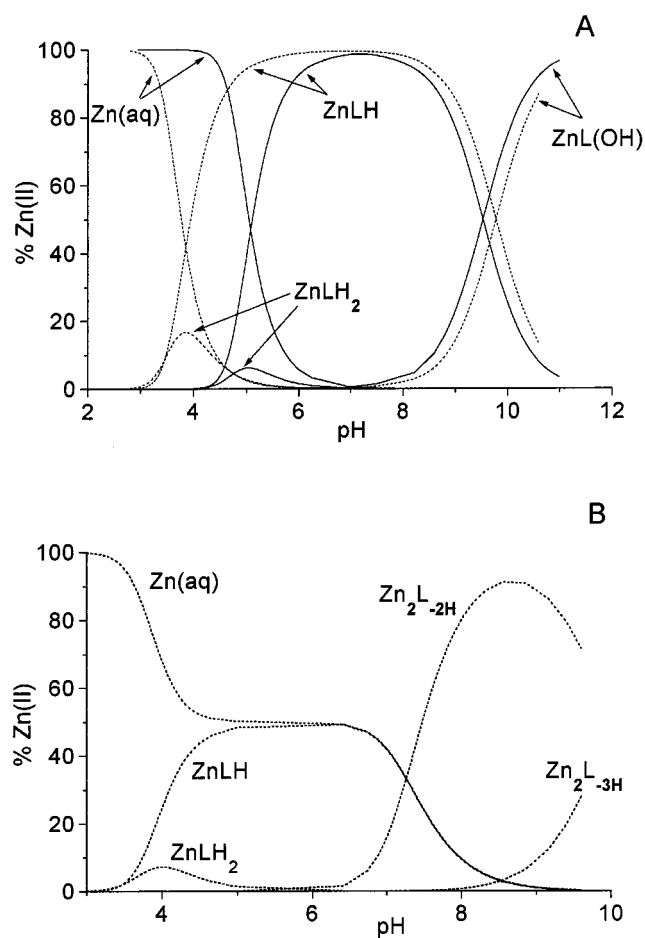


Figure 3. Species distribution curves in the zinc(II)-bimido system at metal-to-ligand ratio 1/1 (A) and 2/1 (B) in water (solid line) and in a 65% (w/w) EtOH-H₂O mixture (dotted line); [Zn] = 3 mM (A) and 1 mM (B)

metal-to-ligand ratio was found to be very sensitive to the solvent used and the background electrolyte. A relatively sharp and well-resolved ¹H NMR spectrum can be obtained by dissolving the crystalline complex **2** in [D₆]DMSO (see supporting information, Figure S1). The signals related to the ligand are spread over a 150 ppm range. The occurrence of the spectrum strongly supports the presence of the dinuclear unit in solution too, allowing magnetic interaction between the metal centres.^[26] In the aqueous solution of copper(II)-bimido ([Cu]/[L] = 2/1) system, without background electrolyte, two strongly overlapping deprotonations are observed pH-metrically between pH 6 and 8, accompanied by the decrease in EPR signal intensity and by a red shift of the *d-d* transition (see supporting information, Figure S2). This indicates the rearrangement of the donor groups in the equatorial plane of copper(II) and the formation of magnetically coupled metal centres. Although no further information is available, the Cu₂L_{-2H} complex formed between pH 6–7, probably has an analogous structure to the crystallographically determined dinuclear complex **2** (the formation of protonation isomers, as in the case of zinc (see later), cannot be ruled out). However, in the

presence of any common background electrolyte precipitation is observed preventing further study.

Complex Formation in a 65% (w/w) Ethanol-Water Mixed Solvent

In the case of the zinc(II)-bimido ([Zn]/[L] = 2/1–1/2) system, solubility problems are overcome by using a 65% (w/w) ethanol-water solvent mixture. This solution is clear in the whole pH range and thus it is suitable for equilibrium and kinetic measurements (see also the experimental section). The p*K* values of bimido are lower than those obtained in aqueous solution (Table 3), according to the somewhat lower permittivity of the solvent. Since the association is more favoured in this medium than in water, the stability of the ZnLH and ZnL complexes, reflected by the basicity corrected stability constants (Table 3), is considerably higher.

At a 2/1 metal-to-ligand ratio, two deprotonations (one per zinc(II) ion) are observed between pH 6.5–8, in a strongly overlapping manner, forming the M₂L_{-2H} species (Figure 3B). A similar observation is mentioned above for copper(II), but in the present case the deprotonation processes take place at higher pH values of ca. 0.7 units. With increasing pH, a further deprotonation is observed (p*K* = 10.0).

The ¹H NMR spectrum of the ZnL species is changed significantly relative to that of the free ligand (Figure 4).

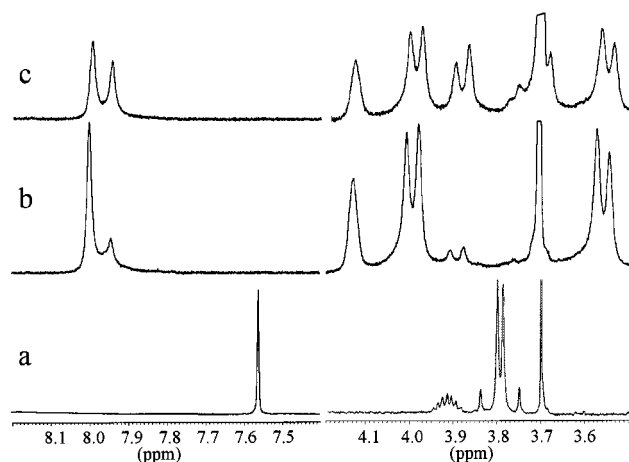


Figure 4. Selected regions of the ¹H NMR spectra measured in the zinc(II)-bimido system in 65% CD₃OD - D₂O at pH = 8.6 with the variation of the metal to ligand ratio. [bimido] = 0.005 M (a) and 0.002 M (b, c). [Zn] = 0.0 M (a), 0.0022 M (b) and 0.004 M (c)

The hydrogens of CH₂, linked to the imidazole rings, become strongly inequivalent and all signals shift upon the coordination. The increasing metal-to-ligand ratio at pH 8.5 induces further characteristic changes on the spectra. A new set of peaks appears, indicating the formation of a complex, Zn₂L_{-2H} according to the pH-metric results, which is in a slow exchange on the NMR timescale. Kinetically inert complexes may originate from the formation of either imidazolate- or alkoxo-bridged metal centres. The chemical shift of the imidazole C2–H protons is, however, weakly influenced by the deprotonation. Metal-promoted

Table 4. ^1H NMR chemical shifts and determined coupling constants (see below the table) for the different species formed in the bimido-zinc(II) system at pH = 8.6 in 75% $\text{CD}_3\text{OD} - \text{D}_2\text{O}$

species	C2-H(im), 2 H	CH-OH, 1 H	$\text{CH}_2\text{-im}$, 2 H+2 H	$\text{CH}_2\text{-CH}$, 2 H+2 H	$\text{CH}_3\text{-im}$, 6 H
free lig.	s, 7.56	m, 3.92 ^[a]	m, 3.81, 3.78 ^[b]	m, 3.27, 3.09 ^{[a],[c]}	s, 2.21
ZnL	s, 8.00	m, 4.13	m, 3.99, 3.56 ^[b]	m, 3.27, 3.09 ^[c]	s, 2.22
$\text{Zn}_2\text{L}_{-2\text{H}}$	s, 7.93	m, 3.75	m, 3.88, 3.70 ^[b]	m, — ^[d] , 2.97 ^[c]	s, 2.13
	s, 7.98	m, 4.13	m, 3.98, 3.55 ^[b]	m, 3.26, 3.08 ^[c]	s, 2.22

^[a] Three bond couplings between CH-OH and the two inequivalent $\text{CH}_2\text{-CH}$ hydrogens: $^3J = 4.7$ and 7.4 Hz. — ^[b] Two bond couplings between the inequivalent $\text{CH}_2\text{-im}$ hydrogens: $^2J = 13.4, 14.0, 15.0$ and 13.8 Hz, respectively. — ^[c] Two bond couplings between the inequivalent $\text{CH}_2\text{-CH}$ hydrogens: $^2J = 12.2, 11.7, 11.2$ and 12.0 Hz, respectively. — ^[d] Chemical shift could not be determined due to the overlapping with the broad solvent signal.

proton loss of the neutral imidazole ring i.e. formation of an imidazolate-bridge, induces an important (more than 1 ppm) shift^[14,16] which is not comparable with the presently observed 0.06 ppm. On the other hand, notable changes appear on the signals of the 2-hydroxypropyl unit, especially concerning the central CH group (Table 4). These facts suggest, that the new set of peaks is related to an alkoxo-bridged dinuclear complex. This complex probably has an analogous structure with the crystallographically determined dinuclear complex **2**. Such a structural motif has recently been found in a dinuclear zinc(II) complex of a four substituted 1,3-diamino-2-propanol derivative.^[27] Complex **2** and $\text{Zn}_2\text{L}_{-2\text{H}}$ are different, however, in their protonation states. The second deprotonation in $\text{Zn}_2\text{L}_{-2\text{H}}$ can be assigned to the proton loss of a metal-bound water molecule.

However, as can be seen from Figure 4, only ca. 45% of the ligand is transformed into the above-mentioned complex at a two-fold metal excess and at pH 8.6, while 55% of the ligand remains as a fast exchanging species. A simple explanation of this behaviour would be the presence of 27.5% free metal ion beside the $\text{Zn}_2\text{L}_{-2\text{H}}$ and ZnL complexes. In the absence of the ligand, however, a well defined $\text{Zn}(\text{OH})_2$ precipitate can be observed above pH 7.0 even at a 0.3 mM metal concentration, which prevents any accurate pH-metric or kinetic study. Since the solution of zinc(II)-bimido complexes ($[\text{Zn}]/[\text{L}] = 2/1$) is clear even at a 7 mM metal concentration, the only plausible explanation for the above observation is the presence of protonation isomers, i.e. two complexes with the same $\text{Zn}_2\text{L}_{-2\text{H}}$ composition. One of them is the above-mentioned alkoxo-bridged complex $\text{Zn}_2(\text{L}_{-1\text{H}})(\text{OH})$ which is in a slow exchange. In the other isomer the metal ions are chelated by two nitrogens and both deprotonations are related to the metal-bound water molecules ($\text{Zn}_2\text{L}(\text{OH})_2$). The ^1H NMR signals of this species is only slightly shifted relative to those of the ZnL complex, since the ligand in both cases coordinates to the metal ion(s) by its four nitrogen donors.

Protonation isomers are generally in a fast mutual exchange but in the present case, the protonation of the alkoxide anion induces rearrangement of the coordination sites, which slows the entire process. The $\text{Zn}_2\text{L}(\text{OH})_2$ complex remains in a fast mutual exchange with ZnL and L.

The further deprotonation around pH 10 results in the formation of $\text{Zn}_2\text{L}_{-3\text{H}}$ species, which is probably better described as $\text{Zn}_2(\text{L}_{-1\text{H}})(\text{OH})_2$.

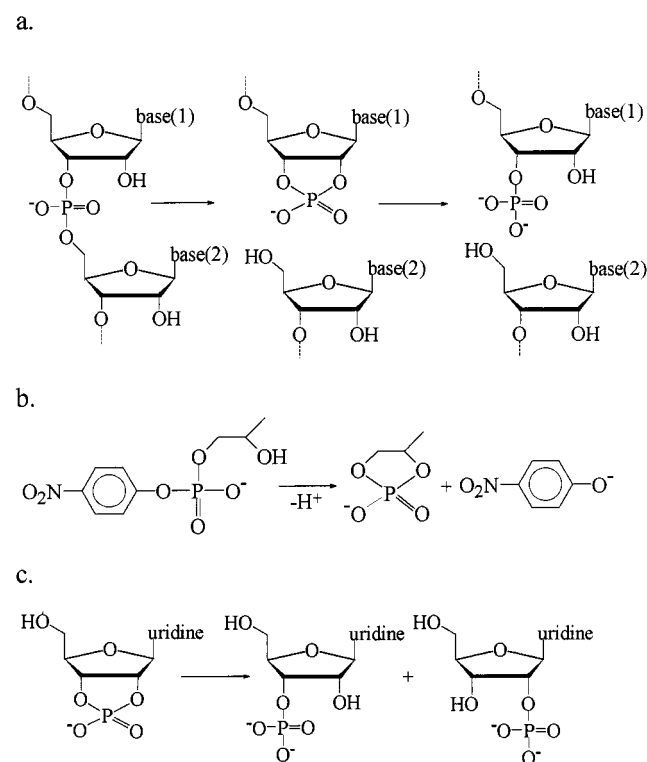
Kinetic Study

The hydrolytic cleavage of RNA is a two-step process: the first step is a transesterification forming a cyclic phosphoester, while the second step is the ring opening.

The hydrolytic activity of the above systems is tested by modelling both steps of RNA hydrolysis i.e. transesterification of hpnp and hydrolysis of 2',3'-cUMP (Scheme 2).

Hydrolytic Activity of the Copper(II)-bimido Complexes

The pH-rate profiles of the transesterification of hpnp and hydrolysis of cUMP, having sigmoidal character, are



Scheme 2. The two-step process of RNA hydrolysis (a) and the used model substrates: b. 2-hydroxypropyl-*p*-nitrophenyl phosphate (hpnp) and c. uridine 2',3'-cyclic monophosphate (2',3'-cUMP). Base(1) and base(2) indicate organic base constituents of RNA

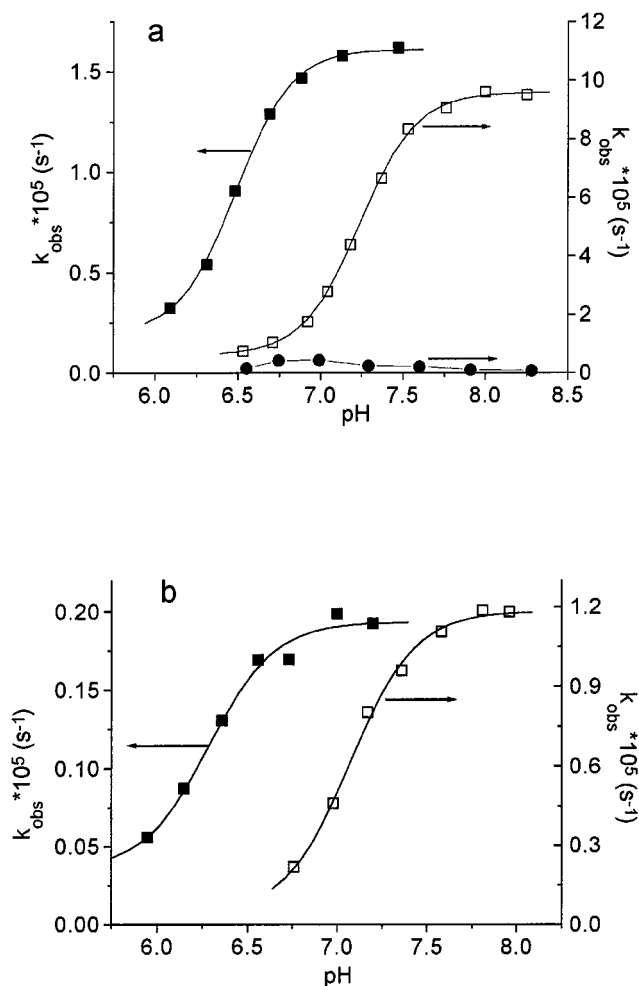


Figure 5a–b. The effect of pH on the observed kinetic data. – a) (■) transesterification of hnpnp by the copper(II)-bimido complexes ($T = 298\text{ K}$, $0.51 \cdot [\text{Cu}] = [\text{L}] = 5 \cdot 10^{-4}\text{ M}$, 0.01 M MES or HEPES, $[\text{hnpnp}] = 5.4 \cdot 10^{-4}\text{ M}$); (□) transesterification of hnpnp by the zinc(II)-bimido complexes (65% (w/w) EtOH–H₂O, $T = 298\text{ K}$, $I = 0.05\text{ M}$, $0.52 \cdot [\text{Zn}] = [\text{L}] = 5.6 \cdot 10^{-4}\text{ M}$, $[\text{hnpnp}] = 5.4 \cdot 10^{-4}\text{ M}$); (●) transesterification of hnpnp by the zinc(II)-ion alone (65% (w/w) EtOH–H₂O, $T = 298\text{ K}$, $I = 0.05\text{ M}$, $[\text{Zn}] = 3.0 \cdot 10^{-4}\text{ M}$, $[\text{hnpnp}] = 9.8 \cdot 10^{-4}\text{ M}$). – b) (■) hydrolysis of cUMP by the copper(II)-bimido complexes ($T = 310\text{ K}$, $0.51 \cdot [\text{Cu}] = [\text{L}] = 5.1 \cdot 10^{-4}\text{ M}$, 0.01 M MES or HEPES, $[\text{cUMP}] = 50\text{ }\mu\text{M}$); (□) hydrolysis of cUMP by the zinc(II)-bimido complexes (65% (w/w) EtOH–H₂O, $T = 310\text{ K}$, $I = 0.05\text{ M}$, $0.52 \cdot [\text{Zn}] = [\text{L}] = 2.1 \cdot 10^{-3}\text{ M}$, $[\text{cUMP}] = 50\text{ }\mu\text{M}$)

shown in Figure 5. In both cases, the observed rate increases between pH 6–7.5, which is parallel with the formation of the $\text{Cu}_2\text{L}_{-2\text{H}}$ species (see also Figure S2), implying its active role in the reaction. However, due to the absence of background electrolyte, a detailed kinetic study was not performed.

Transesterification of hnpnp by the Zinc(II)-Bimido Complexes

The pH-rate profile of the transesterification of hnpnp shows a sigmoidal shape again (Figure 5a). The increasing activity between pH 6.5–8 is parallel with the pH-metrically observed deprotonations at a 2/1 metal-to-ligand ratio (Figure 3b). The pseudo-first order rate constant levels off between pH 8–8.8 and decreases at higher pH (not shown).

The $\text{p}K$ value determined from the kinetic data ($\text{p}K = 7.24$) agrees well with the pH-metric results. For comparative purposes, we also studied the hydrolytic activity of the zinc(II) solution in the absence of bimido (Figure 5a). Due to the formation of a $\text{Zn}(\text{OH})_2$ precipitate above pH 7, the observed rate constants are relatively uncertain. Nevertheless, the free zinc(II) induced rate enhancement is negligible relative to that of zinc(II)-bimido system. All these facts suggest that the hydrolytic activity is related to the $\text{Zn}_2\text{L}_{-2\text{H}}$ species, although no distinction can be made concerning the two protonation isomers since their ratio is independent from pH and concentration. The uncatalysed reaction of hnpnp at pH 8 is relatively slow ($k_{\text{obs,uncat}} = 1.3 \cdot 10^{-7}\text{ s}^{-1}$, half lifetime 62 days) under the conditions used. However, in the presence of 0.54 mM $\text{Zn}_2\text{L}_{-2\text{H}}$ complex at pH 8, the half lifetime decreases to 2 hours. Three turnovers are observed without significant loss of activity at pH 8 when a 3-fold excess of hnpnp is present over the dinuclear complex (0.5 mM).

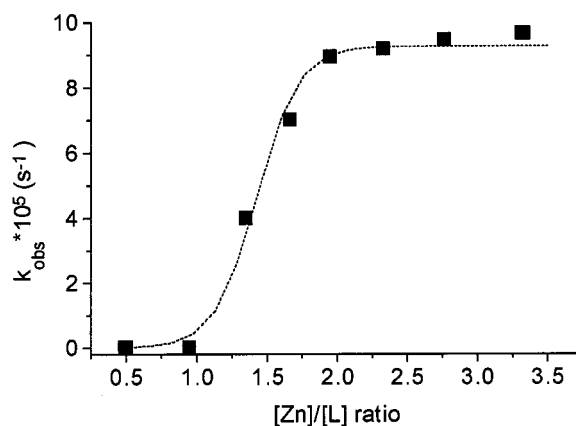


Figure 6. Dependence of the rate of transesterification on the $[\text{Zn}]/[\text{bimido}]$ ratio at constant bimido concentration; pH = 7.98, $[\text{bimido}] = 5.6 \cdot 10^{-4}\text{ M}$

Figure 6 shows the observed pseudo-first order rate constants as a function of the $[\text{Zn}]/[\text{bimido}]$ ratio at constant ligand concentration. The rate is negligible up to equimolar conditions, it sharply increases between a 1/1 and 2/1 ratio and finally levels off at a higher metal excess (where precipitation occurred). This observation provides further argument that the observed activity is a result of the $\text{Zn}_2\text{L}_{-2\text{H}}$ species.

At a constant metal-to-ligand ratio and at pH 7.98, the rate of transesterification linearly depends on the concentration of the $\text{Zn}_2\text{L}_{-2\text{H}}$ complex between $0.2\text{ mM} < [\text{Zn}] < 2\text{ mM}$ (Figure 7). The second order rate constant (k_2) determined from the slope of this plot is $0.186\text{ M}^{-1}\text{ s}^{-1}$. This value is 2.5 times higher than that of the hydroxide ion induced transesterification ($k_{2,\text{OH}} = 0.0745\text{ M}^{-1}\text{ s}^{-1}$), determined between pH 8.8–10.9 in water (in a 65% EtOH–H₂O mixture precipitation occurred using CAPS buffer).

The rate of transesterification is also measured as a function of the substrate concentration (Figure 8). At higher hnpnp concentration, saturation kinetics is observed, implying that the transesterification proceeds through pre-equi-

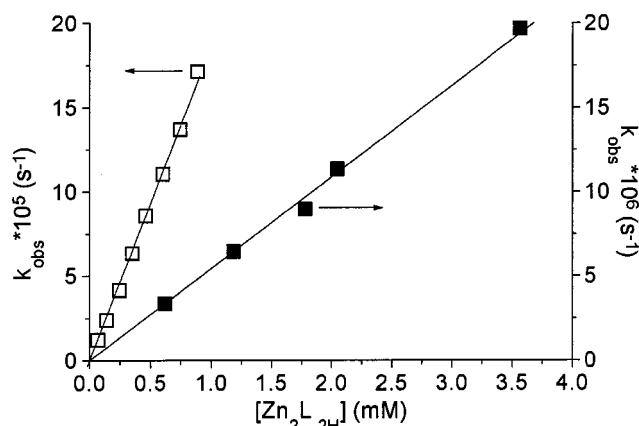


Figure 7. Dependence of the observed pseudo-first order rate constant on the concentration of $[\text{Zn}_2\text{L}_{-2\text{H}}]$ complex. – (□) transesterification of hpnp (65% (w/w) EtOH- H_2O , $T = 298\text{ K}$, $I = 0.05\text{ M}$, $0.52 \cdot [\text{Zn}] = [\text{L}]$, $\text{pH} = 7.98$, $[\text{hpnp}] = 5 \cdot 10^{-4}\text{ M}$); (■) hydrolysis of cUMP (65% (w/w) EtOH- H_2O , $T = 310\text{ K}$, $I = 0.05\text{ M}$, $0.52 \cdot [\text{Zn}] = [\text{L}]$, $[\text{cUMP}] = 50\text{ }\mu\text{M}$)

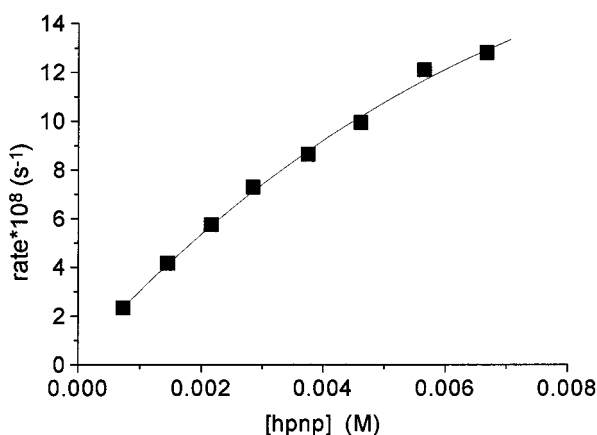
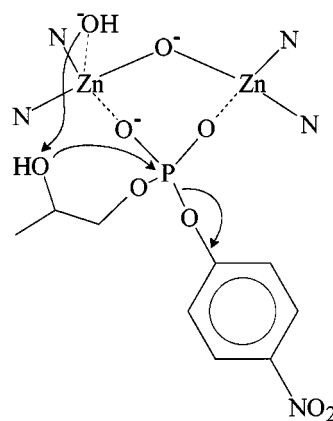


Figure 8. Saturation kinetic experiments for the transesterification of hpnp (65% (w/w) EtOH- H_2O , $T = 298\text{ K}$, $I = 0.05\text{ M}$, $0.52 \cdot [\text{Zn}] = [\text{L}] = 2.1 \cdot 10^{-4}\text{ M}$, $\text{pH} = 7.98$)

libration of an active (catalyst-substrate) complex. The Michaelis-Menten constant (K_M), determined by nonlinear parameter fitting, is 9.1 mM ($K_{\text{ass}} = 1/K_M = 110\text{ M}^{-1}$) and the first order catalytic rate constant (k_{cat}) is $1.52 \cdot 10^{-3}\text{ s}^{-1}$. These values indicate the moderate binding affinity of hpnp to the dinuclear $\text{Zn}_2\text{L}_{-2\text{H}}$ species, but high catalytic activity of this complex. As far as we are aware, the above k_{cat} value is the highest value reported to date for transesterification of hpnp by a zinc(II) complex.

The above experimental data, together with the crystal structure of complex **2**, provide some information on the possible mechanism of the transesterification. The pH-rate profile levels off between pH 8–8.8 (Figure 5.a) parallel with the concentration distribution of the $\text{Zn}_2\text{L}_{-2\text{H}}$ species (Figure 3.b). This means that general base catalysis, activating the nucleophilic $\beta\text{-OH}$ group, is provided mainly by the metal-bound hydroxide ion. However, the second order rate constant of the transesterification by the dinuclear zinc(II) complex is 2.5-fold higher than $k_{2,\text{OH}}$. This implies a bifunctional mechanism for the transesterification, since the nucleophilicity of the metal-bound hydroxide ion is consider-



Scheme 3. The proposed mechanism for hpnp transesterification by the alkoxo-bridged dinuclear complex

ably lower than that of the free OH^- ion. Thus, additional Lewis-acid activation, or in other words metal coordination of the phosphate group, should be considered. Based on the crystal structure of the dinuclear complex **2**, this probably occurs in a $\mu\text{-}1,3$ bridging fashion (Scheme 3). In most cases, such double Lewis-activation is the key feature of highly active dinuclear complexes.^[2,7,8,28]

Since bridging alkoxide anions are not considered to be active as (general-)base catalysts,^[2,4,6,8] the proposed mechanism should be valid for both protonation isomers. Due to the constant ratio of the protonation isomers, no experimental data are available for their individual activity. An overview of the literature data indicates, however, higher hydrolytic activity of rigidly pre-organised bimetallic cores,^[2,29] allowing direct metal-metal cooperation, as compared with the more flexible dinuclear complexes. This would suggest the predominance of the $\text{Zn}_2(\text{L}_{-1\text{H}})(\text{OH})$ isomer in the hydrolytic processes.

Hydrolysis of 2',3'-cUMP

The use of *p*-nitrophenyl phosphates to mimic natural phosphoesterases is not fully justified, since in contrast to biological phosphoesters, the 4-nitrophenolate leaving group does not require electrophilic stabilisation. To mimic the second step of RNA hydrolysis we use the biologically more relevant 2',3'-cUMP, which provides a direct analogy to the natural process (Scheme 2).

The pH-rate profile of 2',3'-cUMP hydrolysis by the dinuclear zinc complex (Figure 5.b) shows similar sigmoidal behaviour as the hpnp transesterification. A pK value of 7.06 can be determined from the kinetic data which is somewhat smaller than the previously determined $\text{pK} = 7.24$. This difference is due to the four-fold increase in the metal concentration and the higher temperature (310 K) used in present case. 2',3'-cUMP is highly resistant to hydrolysis. The second order rate constant^[30] for the hydroxide-catalysed hydrolysis at $37\text{ }^\circ\text{C}$ is ca. $6.5 \cdot 10^{-3}\text{ M}^{-1}\text{ s}^{-1}$. Based on this value, the approximate parameters for the autohydrolysis at pH 8 are $k_{\text{obs,uncat}} = 1\text{--}2 \cdot 10^{-9}\text{ s}^{-1}$ and the half-life time is ca. 11–22 years. In the presence of a 3.6 mM dinuclear zinc(II) complex the half-life time of 2',3'-cUMP is 10

hours at pH 8. Thus, a 3.6 mM zinc complex provides ca. $1\text{--}2\cdot 10^4$ -fold rate acceleration, which is the highest value reported to date for the 2',3'-cUMP hydrolysis promoted by a dinuclear zinc(II) complex. On the other hand, Komiyama's dinuclear zinc(II) complex^[4] hydrolyses ApA with a comparable rate and thus, although no numerical data is given, it probably provides a faster hydrolysis for cyclic monophosphates. We also tested the activity of the dinuclear zinc(II)-bimido complex towards the hydrolysis of UpU. In the presence of a 4 mM dinuclear species and at 310 K, ca. 5% conversion is achieved after 3 days. This suggests an accelerated reaction but the rate is too small for accurate measurement.

The rate of hydrolysis shows first order dependence on the concentration of the $\text{Zn}_2\text{L}_{-2\text{H}}$ species (Figure 7) between $1.2\text{ mM} < [\text{Zn}] < 7.2\text{ mM}$. The second order rate constant determined from the slope is $0.0054\text{ M}^{-1}\text{ s}^{-1}$. This value is close to that of the hydroxide ion (ca. $0.0065\text{ M}^{-1}\text{ s}^{-1}$).

The mechanism of the hydrolysis by the dinuclear complex is probably similar (as depicted in Scheme 3) to the hpnp transesterification. In the present case, however, the metal-bound hydroxide ion may act either as a general base (deprotonating the attacking water molecule) or as a direct nucleophile.

Experimental Section

Materials: Zinc(II) perchlorate (Fluka) solutions were standardised complexometrically. pH metric titrations were performed by Titrisol NaOH standard solution (Merck). HEPES, HEPPS, CHES, CAPS (Aldrich) and MES and 2',3'-cUMP (Sigma) were used without further purification. The barium salt of 2-hydroxypropyl-*p*-nitrophenyl phosphate (hpnp) was prepared according to the literature procedure^[31].

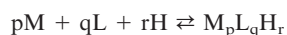
Synthesis of *N,N'*-Bis(5-methylimidazol-4-ylmethyl)-1,3-diaminopropan-2-ol-4 HCl (Bimido): 5-Methylimidazole-4-carboxaldehyde (1.67 g, 15 mmol) and 1,3-diamino-2-propanol (0.7 g, 7.5 mmol) were dissolved in 60 mL of dry methanol. To this solution 1.2 g of sodium borohydride were added in small portions while stirring. After 3 h at room temperature, the reaction was completed by refluxing for 1 h. The methanol solution was then acidified by concentrated hydrochloric acid. The precipitate was filtered, the solution was reduced to 2–3 mL and 30 mL of methanol was added. The precipitate was filtered off again. The solution was evaporated to dryness by codistillation with absolute ethanol. The crude product was recrystallised twice from methanol. Yield: 2 g, 63%. The structure and purity was confirmed by NMR spectroscopy and potentiometry. ¹H NMR (D_2O): $\delta = 8.63$ (s, 2 H, C2–H(im)), 4.43 (s, 4 H, $\text{CH}_2\text{--im}$), 4.34 (m, ³*J* = 4.0 and 11.3 Hz, 1 H, *CH*–OH), 3.30 and 3.16 (m, ²*J* = 15.8 Hz, ³*J* = 4.0 and 11.3 Hz, 2 H + 2 H, *CH*₂–CH) and 2.36 (s, 6 H, $\text{CH}_3\text{--im}$). No other signal was detected.

pH-metric Measurements: The complex formation equilibria were investigated by potentiometric titrations using an automatic titration set including a Dosimat 665 (Metrohm) autoburette, an Orion-710A precision digital pH-meter and an ORION ROSS 8103BN type combined glass electrode. The experimental procedure refer-

ring to the aqueous solution (0.1 M NaClO₄, and $T = 298\pm 0.1$) was described in detail earlier.^[15–17]

In 65% (w/w) ethanol-water mixture the zinc(II)-bimido ($[\text{Zn}]/[\text{L}] = 2/1\text{--}1/2$) solution was clear between pH 2–10 when only buffer was present, but gave slight precipitation using any common inorganic background salt. To avoid this precipitation sodium benzenesulfonate (0.05 M) was used as a background salt and a clear solution, in the used concentration ($[\text{Zn}] = 0.4\text{--}7.0\cdot 10^{-3}\text{ mol dm}^{-3}$) and pH range, was obtained. The pH-meter was calibrated by standard aqueous buffer solutions (pH = 4.01 and 7.0, Mettler–Toledo) and the actual pH in the mixed solvent was then determined by subtracting 0.24 units from the pH-meter reading according to the method of Bates.^[32] The ionisation constant of water determined under the used conditions ($\text{p}K_{\text{w}} = 14.92\pm 0.02$) is in good agreement with that of extrapolated value from the literature data.^[33]

The protonation and the complex formation constants were calculated as the average of 4 and 8 independent titrations (50–80 data points per titration), respectively. The metal-to-ligand ratios were varied from 2:1 to 1:2 with metal-ion concentrations between $5\cdot 10^{-4}$ and $4\cdot 10^{-3}\text{ mol dm}^{-3}$. The species formed in the systems were characterised by the following general equilibrium process



(charges are omitted for simplicity; M denotes the metal ion and L the non-protonated ligand molecule) and the concentration stability constants of these species were calculated by the computer program PSEQUAD.^[34]

X-ray Crystallography: The crystals suitable for X-ray analysis were obtained by the following ways:

[Zn(bimido)Cl]NO₃ (1): Bimido-4 HCl (66 mg, 0.15 mmol) dissolved in 5 mL of dry methanol was neutralised with 4 equivalents of NaOH (in MeOH). $\text{Zn}(\text{NO}_3)_2\cdot 6\text{H}_2\text{O}$ (44.6 mg, 0.15 mmol) was then added. The solution was heated to 50 °C and gently concentrated to 2–3 mL. After slowly cooling the solution to room temperature, colourless crystals were obtained in 2–3 days. Anal. calculated for $\text{C}_{13}\text{H}_{22}\text{ClN}_7\text{O}_4\text{Zn}$: C 35.38, H 4.99, N 22.22; found C 35.08, H 4.91, N 22.42.

[Cu₂(bimido-1H)(DPP)(ClO₄)(CH₃OH)]ClO₄·1/2 H₂O (2): In a similar way, bimido-4 HCl (66 mg, 0.15 mmol) in 5 mL dry methanol was mixed with 6 equivalents of NaOH (in MeOH), diphenylphosphonic acid (32.7 mg, 0.15 mmol) and $\text{Cu}(\text{ClO}_4)_2\cdot 6\text{H}_2\text{O}$ (111.2 mg, 0.3 mmol). After a similar treatment as in **1**, deep blue crystals were obtained. Anal. calculated for $\text{C}_{26}\text{H}_{36}\text{Cl}_2\text{Cu}_2\text{N}_6\text{O}_{14.5}\text{P}$: C 34.94, H 4.03, N 9.41; found C 35.06, H 4.08, N 9.34.

X-ray data were collected on a STOE IPDS diffractometer using Mo-*K*_α-radiation ($\lambda = 0.71073\text{ Å}$) at 213 K with sample-to-plate distance of 70 mm and a scan range from 100 to 301° (**1**) and from 5 to 205° (**2**), with an exposure time of 4 min per 1.5° increment for **1** and 1.3° for **2**. The structures were solved using the direct method^[35] and refined^[36] by full-matrix least square by minimising the function $\sum w(|F_0| - |F_c|)^2$, where F_0 and F_c are the observed and calculated structure factors. Anisotropic thermal parameters were used for all non-hydrogen atoms except for the lattice water oxygen in **2**. Hydrogen atoms were included in the refinement using the riding model. The isotropic thermal parameters for the methyl and hydroxyl protons were refined with 1.5 times, for all other hydrogen atoms with 1.2 times, U_{eq} of the attached atom. H atoms of the lattice water in **2** were not found. The residual electron density on the final difference Fourier map was relatively low for **1**

Table 5. Crystallographic data, details of data collection and structure analysis for complexes **1** and **2**

	1	2
empirical formula	C ₁₃ H ₂₂ ClN ₇ O ₄ Zn	C ₂₆ H ₃₆ Cl ₂ Cu ₂ N ₆ O _{14.5} P
<i>M_r</i>	441.19	893.56
crystal size (mm)	0.24×0.32×0.48	0.16×0.20×0.32
crystal system	monoclinic	triclinic
space group	<i>P</i> 2 ₁ / <i>c</i>	<i>P</i> $\bar{1}$
<i>a</i> (Å)	11.311(2)	7.290(1)
<i>b</i> (Å)	13.299(3)	13.430(3)
<i>c</i> (Å)	12.816(3)	18.090(4)
α , deg	90.00	92.37(3)
β , deg	103.43(3)	97.02(3)
γ , deg	90.00	99.38(3)
<i>V</i> (Å ³)	1865.26	1730.9(6)
density calcd. (g cm ⁻³)	1.571	1.714
<i>Z</i>	4	2
<i>T</i> (K)	213(2)	213(2)
Θ range for data collection	4.05–26.05°	4.71–26.12°
index ranges	–13 ≤ <i>h</i> ≤ 12, –16 ≤ <i>k</i> ≤ 16, –15 ≤ <i>l</i> ≤ 15	–8 ≤ <i>h</i> ≤ 8, –16 ≤ <i>k</i> ≤ 16, –22 ≤ <i>l</i> ≤ 22
μ (mm ⁻¹)	1.490	1.506
<i>F</i> (000)	885	914
reflections collected/unique	14864/3657 [<i>R</i> (int) = .00752]	13672/6281 [<i>R</i> (int) = .1060]
number of parameters	235	466
final <i>R</i> indices (all data) ^[a]	<i>R_f</i> = 0.0305, <i>wR</i> 2 = 0.0750	<i>R_f</i> = 0.1033, <i>wR</i> 2 = 0.1956
final <i>R</i> indices [<i>I</i> > 2σ(<i>I</i>)]	<i>R_f</i> = 0.0314, <i>wR</i> 2 = 0.0836	<i>R_f</i> = 0.0657, <i>wR</i> 2 = 0.1656
weighting scheme ^[b]	1/[σ ² (<i>F_o</i> ²) + (0.0328 <i>P</i>) ² + 1.34 <i>P</i>]	1/[σ ² (<i>F_o</i> ²) + (0.0897 <i>P</i>) ² + 2.83 <i>P</i>]
goodness of fit on <i>F</i> ²	1.046	1.050
diff. Fourier peaks, min/max	–0.32/0.33	–0.67/1.56

^[a] $R_1 = \Sigma ||F_o| - |F_c|| / \Sigma |F_o|$, $wR_2 = [\Sigma w(F_o^2 - F_c^2)^2 / \Sigma w(F_o^2)^2]^{1/2}$. – ^[b] $P = [\max(F_o^2, 0) + 2F_c^2]/3$

(0.33–0.32 e/Å³), while in case of **2** the two highest peaks were found to be 1.56 and 0.85 e/Å³, associated with Cl(1). The thermal parameters of the complex cation in **2** were well behaved, but those of the perchlorate ions and lattice water were relatively large. Attempts to improve the model for the disordered Cl(1) perchlorate ion resulted in a lower final agreement index and residual electron density, but a higher thermal parameter for one of the disordered perchlorate oxygen and thus were unsatisfactory. Further data collection parameters and information related to the structure refinement are collected in Table 5.

Crystallographic data (excluding structure factors) for the structures reported in this paper have been deposited with the Cambridge Crystallographic Data Center as supplementary publication no. CCDC-127400 (**1**) and CCDC-135915 (**2**). Copies of the data can be obtained free of charge on application to CCDC, 12 Union Road, Cambridge CB2 1EZ, UK (Fax: +44–1223/336–033; E-mail: deposit@ccdc.cam.ac.uk).

NMR Spectroscopic Measurements: The ¹H NMR spectroscopic measurements were performed on a Bruker AM-360 spectrometer, operating at room temperature. The chemical shifts have been given as relative shifts from DSS (the sodium salt of 4,4-dimethyl-4-silapentane-1-sulfonate) using dioxane as the internal reference (3.7 ppm from DSS).

Kinetic Measurements. – Transesterification of hpnp: The reaction was followed in 65% (w/w) ethanol-water (*I* ≈ 0.05 M with 0.02 M buffer (HEPES, HEPPS or CHES) and 0.03 M sodium benzenesulfonate). The increase in the absorbance maximum at 400 nm of the *p*-nitrophenolate anion (ϵ = 18900) was monitored. The p*K* of *p*-nitrophenol and the buffers were determined independently for our conditions (p*K* = 8.04±0.01 (hpnp), 7.13±0.01 (HEPES), 7.56±0.01 (HEPPS), 8.80±0.01 (CHES)). The initial concentration of hpnp varied from 0.4 mM to 7 mM. The initial slope method (≤ 4% conversion) was used to determine the pseudo first order rate constants. The reported data are the average of triplicate measurements (reproducibility ≤ 10%).

Hydrolysis of 2',3'-cUMP: Kinetic data were measured by hydrolysing the 2',3'-cUMP in a 65% (w/w) ethanol-water mixture (buffer concentration 0.05 M) in the presence of zinc(II)-bimido complexes at 310 K and by analysing the unchanged substrate and products (uridine-2'-phosphate, uridine-3'-phosphate and a small amount of uridine) by HPLC. The pH of the reaction solutions were measured at 298 K, before initiation of the hydrolysis. The initial substrate concentration was 5·10⁻⁴ mol dm⁻³. Ten aliquots of the reaction solutions were periodically taken up in each run. The progress of the reaction was stopped by mixing 0.1 mL aliquot with equal amount of eluent used for HPLC (0.025 mol dm⁻³ acetate buffer, pH = 4.3, containing 0.1 mol dm⁻³ ammonium chloride). The sample was then injected into the HPLC column. The chromatographic separations were carried out on a Merck HPLC system. The column was a Lichrospher 100 RP-18 (150 × 4 mm i.d.), 5 mm particle size (Merck). The UV detection was carried out at 260 nm. The hydrolysis was followed for c.a. three half-lives, by observing the disappearance of uridine-2',3'-cyclic monophosphate. In all cases pseudo first-order kinetics were observed. The rate constants (*k*_{obs}) were obtained from the plots of the ratio of the peaks area: [substrate]/([substrate]+[product]) (*A_t*) vs time fitted by the standard exponential model (*A_t* = *A₀*exp(–*k*_{obs}·*t*)), using a nonlinear least-squares treatment. The reported data are the average of duplicate measurements (reproducibility ≤ 10%).

Acknowledgments

T. G. thanks the Alexander von Humboldt Foundation for a research fellowship. This work was supported by the Deutsche Forschungsgemeinschaft and by the Hungarian Research Foundation (Project No. T025114).

[1] [1a] W. N. Lipscomb, N. Sträter, *Chem. Rev.* **1996**, *96*, 2375–2433. – [1b] D. E. Wilcox, *Chem. Rev.* **1996**, *96*, 2435–2458.

[2] For reviews on dinuclear functional models see: [2a] R. Krämer, T. Gajda, *Perspectives on Bioinorganic Chemistry*, vol. 4 (Ed.: R.

- W. Hay, J. R. Dilworth, K. Nolan), JAI Press Inc., **1999**, pp. 207–240. — ^[2b] J. Chin, *Curr. Opin. Biol.* **1998**, *1*, 514–521. — ^[2c] N. H. Williams, B. Takasaki, M. Wall, J. Chin, *Acc. Chem. Res.* **1999**, *32*, 485–493.
- ^[3] W. H. Chapman Jr., R. Breslow, *J. Am. Chem. Soc.* **1995**, *117*, 5462–5469.
- ^[4] M. Yashiro, A. Ishikubo, M. Komiyama, *J. Chem. Soc., Chem. Commun.* **1995**, 1793–1794.
- ^[5] P. Molenveld, S. Kapsabelis, J. F. J. Engbersen, D. N. Reinhoudt, *J. Am. Chem. Soc.* **1997**, *119*, 2948–2949.
- ^[6] T. Koike, M. Inoue, E. Kimura, M. Shiro, *J. Am. Chem. Soc.* **1996**, *118*, 3091–3099.
- ^[7] D. Wahnnon, R. C. Hynes, J. Chin, *J. Chem. Soc., Chem. Commun.* **1994**, 1441–1442.
- ^[8] M. Wall, R. C. Hynes, J. Chin, *Angew. Chem.* **1993**, *105*, 1696–1697; *Angew. Chem. Int. Ed. Engl.* **1993**, *32*, 1633–1635.
- ^[9] M. J. Young, J. Chin, *J. Am. Chem. Soc.* **1995**, *117*, 10577–10578.
- ^[10] S. Liu, A. D. Hamilton, *Bioorg. Med. Chem. Lett.* **1997**, *7*, 1779–1784.
- ^[11] S. Liu, Z. Lou, A. D. Hamilton, *Angew. Chem.* **1997**, *109*, 2794–2796; *Angew. Chem. Int. Ed. Engl.* **1997**, *36*, 2678–2680.
- ^[12] ^[12a] P. Hurst, B. K. Takasaki, J. Chin, *J. Am. Chem. Soc.* **1996**, *118*, 9982–9983. — ^[12b] K. Matsumura, M. Komiyama, *J. Biochem.* **1997**, *122*, 387–394.
- ^[13] P. Molenveld, J. F. Engbersen, H. Kooijman, A. L. Spek, D. N. Reinhoudt, *J. Am. Chem. Soc.* **1998**, *120*, 6726–6737.
- ^[14] I. Török, T. Gajda, B. Gyurcsik, G. K. Tóth, A. Péter, *J. Chem. Soc., Dalton Trans.* **1998**, 1205–1212.
- ^[15] T. Gajda, B. Henry, J.-J. Delpuech, *J. Chem. Soc., Dalton Trans.* **1993**, 1301–1306.
- ^[16] T. Gajda, B. Henry, J.-J. Delpuech, *Inorg. Chem.* **1995**, *34*, 2455–2460.
- ^[17] T. Gajda, B. Henry, A. Aubry, J.-J. Delpuech, *Inorg. Chem.* **1996**, *35*, 586–593.
- ^[18] T. P. E. Auf der Heyde, L. R. Nassimbeni, *Acta Crystallogr. Sect. B*, **1984**, *B40*, 582–589.
- ^[19] see for example N. W. Alcock, A. Berry, P. Moore, *Acta Crystallogr. Sect. C*, **1984**, *C48*, 16–17.
- ^[20] E. E. Bernarducci, P. K. Bharadwaj, R. A. Lalancette, K. Krogh-Jespersen, J. A. Potenza, H. J. Schugar, *Inorg. Chem.* **1983**, *22*, 3911–3920.
- ^[21] ^[21a] V. McKee, M. Zvagulis, J. D. Dagdigan, M. G. Patch, C. A. Reed, *J. Am. Chem. Soc.* **1984**, *106*, 4765–4772. — ^[21b] J. H. Satcher, Jr., M. W. Droegge, T. J. R. Weakley, R. T. Taylor, *Inorg. Chem.* **1995**, *34*, 3317–3328. — ^[21c] H. Nie, S. M. J. Aubin, M. S. Mashuta, R. A. Porter, J. F. Richardson, D. N. Hendrickson, R. M. Buchanan, *Inorg. Chem.* **1996**, *35*, 3325–3334.
- ^[22] ^[22a] W. Mazurek, B. J. Kennedy, K. S. Murray, M. J. O'Connor, J. R. Rodgers, M. S. Snow, A. G. Wedd, P. R. Zwack, *Inorg. Chem.* **1985**, *24*, 3258–3264. — ^[22b] Y. Nishida, S. Kida, *J. Chem. Soc., Dalton Trans.* **1986**, 2633–2640. — ^[22c] M. Mikuriya, Y. Hatano, E. Asato, *Chem. Lett.* **1996**, 849–850. — ^[22d] S. T. Frey, N. M. Murthy, S. T. Weintraub, L. K. Tomphson, K. D. Karlin, *Inorg. Chem.* **1997**, *36*, 956–957. — ^[22e] T. N. Sorrel, C. J. O'Connor, O. P. Anderson, J. H. Reibenspies, *J. Am. Chem. Soc.* **1985**, *107*, 4199–4206.
- ^[23] D. W. Gruenwedel, *Inorg. Chem.* **1968**, *7*, 495–501.
- ^[24] D. C. Weatherburn, E. J. Billo, J. P. Jones, D. W. Margerum, *Inorg. Chem.* **1970**, *9*, 1557–1559.
- ^[25] P. Huber, R. Griessen, H. Sigel, *Inorg. Chem.* **1971**, *10*, 945–947.
- ^[26] V. Clementi, C. Luchinat, *Acc. Chem. Res.* **1998**, *31*, 351–361.
- ^[27] S. J. Brundenell, L. Spiccia, D. C. R. Hockless, E. R. T. Tiekink, *J. Chem. Soc., Dalton Trans.* **1999**, 1475–1481.
- ^[28] N. H. Williams, J. Chin, *Chem. Commun.* **1996**, 131–132.
- ^[29] J. S. Seo, N.-D. Sung, R. C. Hynes, J. Chin, *Inorg. Chem.* **1996**, *35*, 7472–7473.
- ^[30] H. I. Abrash, C.-C. S. Cheung, C. Davis, *Biochemistry* **1967**, *6*, 1298–1308.
- ^[31] D. M. Brown, D. A. Usher, *J. Chem. Soc.* **1965**, 6558–6565.
- ^[32] R. G. Bates *Determination of pH*, 2nd ed., John Wiley & Sons, New York, **1964**, pp. 226–227.
- ^[33] E. M. Wooley, D. G. Hurkot, L. G. Hepler, *J. Phys. Chem.* **1970**, *74*, 3908–3916.
- ^[34] L. Zékány, I. Nagypál, in *Computational Methods for the Determination of Formation Constants*, Ed. D. J. Leggett, Plenum, New York, **1991**.
- ^[35] G. M. Sheldrick, SHELXS-86, Program for Crystal Structure Solution; Universität Göttingen, **1986**.
- ^[36] G. M. Sheldrick, SHELXL-97, Program for Crystal Structure Refinement; Universität Göttingen, **1997**.

Received October 25, 1999
[199377]